

# A Novel Methodology for Adaptive Wave Filtering of Marine Vessels: Theory and Experiments\*

Vahid Hassani\*

Vahid.Hassani@marintek.sintef.no

António M. Pascoal\*\*

antonio@isr.ist.utl.pt

Asgeir J. Sørensen\*\*\*

asgeir.sorensen@ntnu.no

**Abstract**—This paper addresses a filtering problem that arises in the design of dynamic positioning systems for ships and offshore rigs subjected to the influence of sea waves. The vessel's dynamic model adopted captures the sea state as an uncertain parameter. The proposed adaptive Wave Filtering (WF) consists of a recursive optimization procedure which seeks to identify the dominant wave frequency (the uncertain parameter) by minimizing an appropriate defined performance index. The estimated dominant wave frequency is used to identify the sea condition, based on which adaptive wave filtering (using a Kalman filter) is performed for dynamic positioning purposes. The adaptive WF enables the DP system to operate in different operational conditions and hence, it is a step forward to a so-called all-year marine DP system. The results are experimentally verified by model testing a DP operated ship, the Cybership III, under different sea conditions, in a towing tank equipped with a hydraulic wave maker.

## I. INTRODUCTION

The advent of offshore exploration and exploitation at an unprecedented scale has brought about increasing interest in the development of dynamic positioning (DP) systems for surface vessels. As a consequence, the number of vessels whose position is regulated by means of DP systems has increased significantly during the last decades. In deep waters, Jack-up barges and anchoring systems cannot be used economically and therefore DP systems are also needed to keep the position and heading of marine structures within pre-specified excursion limits under expected weather windows. Early DP systems were implemented using PID controllers. In order to restrain thruster trembling caused by the wave-induced motion components, notch filters in cascade with low pass filters were used with the controllers. However, notch filters restrict the performance of closed-loop systems

because they introduce phase lag around the crossover frequency, which in turn tends to decrease phase margin. An improvement in performance was achieved by exploiting more advanced control techniques based on optimal control and Kalman filtering (KF) theory, see [1]. These techniques were later modified and extended in [2]–[9]. For a survey of dynamic positioning control systems, see [7]–[10] and the references therein. One of the most fruitful concepts introduced in the course of the body of work referred above was that of wave filtering, together with the strategy of modeling the total vessel motion as the superposition of low-frequency (LF) vessel motion and wave-frequency (WF) motions. It was further recognized that in order to reduce the mechanical wear and tear of the propulsion system components, in small to high sea states, the estimates entering the DP control feedback loop should be filtered by using a so-called wave filtering technique so as to prevent excessive control activity in response to WF components. Furthermore, only the slowly-varying disturbances should be counterbalanced by the propulsion system, whereas the oscillatory motion induced by the waves (1st-order wave induced loads) should not enter the feedback control loop. To this effect, DP control systems should be designed so as to react to the low frequency forces on the vessel only. In practice, position and heading measurements are corrupted not only by sensor noise but also by colored noise caused by wind, waves, and ocean currents. Moreover, in general the measurements of the vessel's velocity are not available; thus the need for an observer to estimate the velocity from corrupted measurements of position and heading and achieve wave filtering and “separate” the LF and WF position and heading estimates (see [11] for details).

In [4], WF filtering was done by exploiting the use of KF theory under the assumption that the kinematic equations of the ship's motion can be linearized about a set of predefined constant yaw angles (36 operating points in steps of 10 degrees, covering the whole heading envelope); this is necessary when applying linear KF theory and gain scheduling techniques. However, global exponential stability (GES) of the complete system cannot be guaranteed. In [12], a nonlinear observer with wave filtering capabilities and bias estimation was designed using passivity. The sea state may undergo large variations and therefore the observer in charge of reconstructing the LF motion should adapt to the sea state itself; adaptive WF and DP were introduced in [5]–[10], [12], where adaptation to sea state change was introduced.

In this paper, inspired by previous pioneering work on DP systems, a modified model for wave filtering, proposed in

\*This work was supported in part by projects MORPH (EU FP7 under grant agreement No. 288704) and the FCT [PEst-OE/EEI/LA0009/2011] and was carried cooperatively by the Norwegian Marine Technology Research Institute (MARINTEK), LARSyS-Instituto Superior Técnico (IST), Technical University of Lisbon, Portugal, and the Centre for Autonomous Marine Operations and Systems (AMOS); the Norwegian research council is acknowledged as sponsor of MARINTEK and AMOS.

\*Vahid Hassani is with the Norwegian Marine Technology Research Institute (MARINTEK), Trondheim, Norway.

\*\*António M. Pascoal is with the Laboratory of Robotics and Systems in Engineering and Science (LARSyS), Instituto Superior Técnico (IST), University of Lisbon, Portugal. He is also an Adjunct Scientist with the National Institute of Oceanography (NIO), Goa, India.

\*\*\*Asgeir J. Sørensen is with the Centre for Autonomous Marine Operations and Systems (AMOS) and Dept. of Marine Technology, Norwegian Univ. of Science and Technology, Trondheim, Norway.

[7]–[9], is used. Based on the adopted model we propose the use of an adaptive wave filter coupled with a parameter identification technique. To this effect, a KF based on an initial value for the uncertain parameter is formed and a performance index is defined to evaluate the performance of the wave filter. Minimization of the performance index over the uncertain parameter is studied and the gradient of the performance index (with respect to the uncertain parameter) is computed. A new estimate for the uncertain parameter is computed and the KF is tuned for the new estimate of the uncertain parameter accordingly. The main emphasis of the paper is on the new parameter identification for WF; however, for the sake of completeness, in the numerical simulations (and practical model tests) a multivariable PID is used to control the position of the vessel.

The structure of the paper is as follows. Section II proposes a linear representative vessel model. Section III introduces the proposed parameter identification technique. It also reviews the basic structure of a Kalman wave filter. Analytic and computational details required to implement the proposed parameter identification technique are described in section IV. In section V, a short description of the model test vessel, Cybership III, and experimental results of model tests are presented. Conclusions and suggestions for future research are summarized in Section VI.

## II. LINEAR MODEL OF THE DP VESSEL

In what follows, the vessel model that is by now standard<sup>1</sup> is presented. See for example [7], [12]. The model admits the realization

$$\dot{\xi}_W = A_W(\omega_0)\xi_W + E_W w_W \quad (1)$$

$$\eta_W = R(\psi_L)C_W\xi_W \quad (2)$$

$$\dot{b} = -T^{-1}b + E_b w_b \quad (3)$$

$$\dot{\eta}_L = R(\psi_L)\nu \quad (4)$$

$$M\dot{\nu} + D\nu = \tau + R^T(\psi_{tot})b \quad (5)$$

$$\eta_{tot} = \eta_L + \eta_W \quad (6)$$

$$\eta_y = \eta_{tot} + v, \quad (7)$$

where (1) and (2) capture the 1st-order wave induced motions in surge, sway, and yaw; equation (3) represents the 1st-order Markov process approximating the unmodelled dynamics and the slowly varying environmental forces (in surge and sway) and torques (in yaw) due to waves (2nd order wave induced loads), wind, and currents. The latter are given in earth fixed coordinates but expressed in body-axis. In the above,  $\eta_W \in \mathbb{R}^3$  is the vessel's WF motion due to 1st-order wave-induced disturbances, consisting of WF position  $(x_W, y_W)$  and WF heading  $\psi_W$  of the vessel;  $w_W \in \mathbb{R}^3$  and

$w_b \in \mathbb{R}^3$  are zero mean Gaussian white noise vectors, and

$$A_W = \begin{bmatrix} 0_{3 \times 3} & I_{3 \times 3} \\ -\Omega_{3 \times 3} & -\Lambda_{3 \times 3} \end{bmatrix}, \quad E_W = \begin{bmatrix} 0_{3 \times 1} \\ I_{3 \times 1} \end{bmatrix},$$

$$C_W = [0_{3 \times 3} \quad I_{3 \times 3}],$$

with

$$\Omega = \text{diag}\{\omega_{01}^2, \omega_{02}^2, \omega_{03}^2\},$$

$$\Lambda = \text{diag}\{2\zeta_1\omega_{01}, 2\zeta_2\omega_{02}, 2\zeta_3\omega_{03}\},$$

where  $\omega_0 = [\omega_{01} \ \omega_{02} \ \omega_{03}]^T$  and  $\zeta_i$  are the Dominant Wave Frequency (DWF) and relative damping ratio, respectively. Matrix  $T = \text{diag}(T_x, T_y, T_\psi)$  is a diagonal matrix of positive bias time constants and  $E_b \in \mathbb{R}^{3 \times 3}$  is a diagonal scaling matrix. Vector  $\eta_L \in \mathbb{R}^3$  consists of low frequency (LF), earth-fixed position  $(x_L, y_L)$  and LF heading  $\psi_L$  of the vessel relative to an earth-fixed frame,  $\nu \in \mathbb{R}^3$  represents the velocity vector decomposed in a vessel-fixed reference, and  $R(\psi_L)$  is the standard orthogonal yaw angle rotation matrix (see [11] for complete details). Equation (5) describes the vessels's LF motion at low speed (see [11]), where  $M \in \mathbb{R}^{3 \times 3}$  is the generalized system inertia matrix including zero frequency added mass components,  $D \in \mathbb{R}^{3 \times 3}$  is the linear damping matrix, and  $\tau \in \mathbb{R}^3$  is a control vector of generalized forces generated by the propulsion system, that is, the main propellers aft of the ship and thrusters which can produce surge and sway forces as well as a yaw moment. Vector  $\eta_{tot} \in \mathbb{R}^3$  describes the vessel's total motion, consisting of total position  $(x_{tot}, y_{tot})$  and total heading  $\psi_{tot}$  of the vessel. Finally, (7) represents the position and heading measurement equation, with  $v \in \mathbb{R}^3$  a zero-mean Gaussian white measurement noise.

From (1)-(6), using practical assumptions, a linear model with parametric uncertainty was obtained in [8] as follows:

$$\dot{\xi}_W = A_W(\omega_0)\xi_W + E_W w_W \quad (8)$$

$$\eta_W^b = C_W\xi_W \quad (9)$$

$$\dot{b}^p = -T^{-1}b^p + w_b^f \quad (10)$$

$$\dot{\eta}_L^p = \nu \quad (11)$$

$$M\dot{\nu} + D\nu = \tau + b^p \quad (12)$$

$$\eta_y^f = \eta_L^p + \eta_W^b \quad (13)$$

where  $\eta_W^b$  are WF components of motion in the body-coordinate axis,  $w_b^f$  and  $\eta_y^f$  are a new modified disturbance and a modified measurement defined by  $w_b^f = R^T(\psi_y)E_b w_b$  and  $\eta_y^f = R^T(\psi_y)\eta_y$ , respectively,  $\omega_0$  is parametric uncertainty, and matrix  $S$  is given by

$$S = \begin{bmatrix} 0 & 1 & 0 \\ -1 & 0 & 0 \\ 0 & 0 & 0 \end{bmatrix}.$$

The equations describing the kinematics and the dynamics of the vessel can be represented in the following standard form for multiple-input-multiple-output (MIMO) linear plant models:

$$\dot{x}(t) = A(\omega_0)x(t) + Bu(t) + Gw(t), \quad (14a)$$

$$y(t) = Cx(t) + v(t), \quad (14b)$$

<sup>1</sup>The model described by (1)-(6) has minor differences with respect to the ones normally available in the literature. While in most of the literature the WF components of motion are modeled in a fixed-earth frame, in this paper the WF motion is modeled in body-frame. The reader is referred to [7] for details and improvements of the present model.

where  $x(t) = [\xi_W^T \ b^p T \ \eta_L^p T \ \nu^T]^T \in \mathbb{R}^{15}$  denotes the state of the system,  $u(t) = M^{-1}\tau \in \mathbb{R}^3$  its control input,  $y(t) = \eta_y^f \in \mathbb{R}^3$  its measured noisy output,  $w(t) = [w_W^T \ w_b^f T]^T \in \mathbb{R}^6$  an input plant disturbance that cannot be measured, and  $v(t) \in \mathbb{R}^3$  is the measurement noise. The equations in (14) are simply a compact way of presenting equations in (8)-(13);  $A(\omega_0)$ ,  $B$ ,  $G$  and  $C$  are defined in the obvious manner. Table I shows the definition of the sea conditions characterized by the DWF. The sea conditions are associated with the particular model of offshore supply vessel that is used in our study. We assume that DWF lies in the interval  $[0.39 \ 1.8]^1$

TABLE I  
DEFINITION OF SEA STATES FROM [13]

| Sea States    | DWF                | Significant Wave Height |
|---------------|--------------------|-------------------------|
|               | $\omega_0$ (rad/s) | $H_s$ (m)               |
| Calm Seas     | $> 1.11$           | $< 0.1$                 |
| Moderate Seas | $[0.74 \ 1.11]$    | $[0.1 \ 1.69]$          |
| High Seas     | $[0.53 \ 0.74]$    | $[1.69 \ 6.0]$          |
| Extreme Seas  | $< 0.53$           | $> 6.0$                 |

that covers calm, moderate, high and extreme sea conditions.

### III. PROBLEM FORMULATION

This section introduces a class of adaptive observers for uncertain linear dynamic systems in a stochastic setting. Consider the discretized plant model<sup>2</sup>

$$x(t+1) = A_\theta x(t) + Bu(t) + G_\theta w(t), \quad (15a)$$

$$y(t) = C_\theta x(t) + v(t), \quad (15b)$$

where  $x(t) \in \mathbb{R}^n$  denotes the state of the system,  $u(t) \in \mathbb{R}^m$  its control input,  $y(t) \in \mathbb{R}^q$  its measured noisy output,  $w(t) \in \mathbb{R}^r$  an input plant disturbance that can not be measured, and  $v(t) \in \mathbb{R}^q$  is the measurement noise. Vectors  $w(t)$  and  $v(t)$  are zero-mean, mutually independent white Gaussian sequences, with covariances  $cov[w(t); w(\tau)] = Q\delta_{t\tau}$  and  $cov[v(t); v(\tau)] = R\delta_{t\tau}$ , respectively. The initial condition  $x(0)$  of (15a) is a Gaussian random vector with mean and covariance given by  $E\{x(0)\} = 0$  and  $E\{x(0)x^T(0)\} = P(0)$ . The matrices  $A_\theta$ ,  $G_\theta$ , and  $C_\theta$  contain *unknown constant parameters* denoted by vector  $\theta \in \Theta \subset \mathbb{R}^l$  where  $\Theta$  is some compact set. If  $\theta$  were fixed and known, the standard KF [14] would provide optimal estimation of the states,  $\hat{x}(t)$ , given by

$$\begin{aligned} \hat{x}_\theta(t+1|t) &= [A_\theta - A_\theta H_\theta(t)C_\theta] \hat{x}_\theta(t|t-1) + Bu(t) \\ &\quad + A_\theta H_\theta(t)y(t) \end{aligned} \quad (16a)$$

$$H_\theta(t) = \Sigma_\theta(t|t-1)C_\theta^T S_\theta^{-1}(t) \quad (16b)$$

$$S_\theta(t) = C_\theta \Sigma_\theta(t|t-1)C_\theta^T + R \quad (16c)$$

$$\begin{aligned} \Sigma_\theta(t+1|t) &= A_\theta \Sigma_\theta(t|t-1)A_\theta^T + G_\theta Q G_\theta^T \\ &\quad - A_\theta H_\theta(t)S_\theta(t)H_\theta^T(t)A_\theta^T, \end{aligned} \quad (16d)$$

<sup>1</sup>We use the same interval for DWF in surge, sway and yaw.

<sup>2</sup>In order to consider more general class of LTI systems, in this section, the plant model (14) is changed to (15) so that parametric uncertainties enter the  $G$  and  $C$  matrices.

where  $[A_\theta, G_\theta]$  and  $[A_\theta, C_\theta]$  are assumed to be stabilizable and detectable. In practice, due to unmodelled dynamics, uncertain parameter values, etc., the actual system and the model used for the KF are not identical. For these reasons, it is necessary to evaluate the performance of a mismatched KF, (a KF designed based on a model that is different from the actual system). Let us consider the case where the exact value of the uncertain parameter is not known and a KF with parametric mismatch, designed assuming  $\theta = \theta_i$ , is used for the estimation. In [15] a steady state performance index is introduced which computes the performance degradation of KF in presence of parametric mismatch, between the true model and the KF, as

$$\Gamma_{\theta_n}^{\theta_*} \equiv +\frac{1}{2} \log(|S_{\theta_n}|) + \frac{1}{2} tr(S_{\theta_n}^{-1} \mathfrak{S}_{\theta_n}^{\theta_*}), \quad (17)$$

where  $\theta_*$  is the exact value of uncertain parameter in the plant and  $\theta_n$  is the nominal value of the uncertain parameter used in designing the KF. Denote by  $S_\theta$  the steady state covariance matrix of residuals in the KF ( $\lim_{t \rightarrow \infty} S_{\theta_n}(t)$ ) given by (16c) as  $t \rightarrow \infty$ ; let  $\mathfrak{S}_{\theta_n}^{\theta_*}$  be the steady state covariance of the residuals in KF tuned for  $\theta_n$  while the true parameter in the plant is  $\theta_*$ . The performance index introduced in (17) is closely related to Baram Proximity Measure (BPM), see [15], [16] for more information on the BPM. The BPM is used to design a bank of KFs in multiple model adaptive estimation and control methodologies [9], [15]. In [17], a new time varying performance index is presented to assess the estimation performance of the KFs in multiple model robust adaptive control methodology, as follows:

$$\mu_\theta(t) := \frac{1}{2} \sum_{\tau=1}^{\tau=t} [\tilde{y}_\theta^T(\tau) S_\theta^{-1}(\tau) \tilde{y}_\theta(\tau) + \log |S_\theta(\tau)|], \quad (18)$$

where  $\tilde{y}_\theta(t) = y(t) - C_\theta \hat{x}_\theta(t|t-1)$  is the output estimation error (residual). It is further shown in [17] that  $\mu_\theta(t)$  converges to the BPM as  $t \rightarrow \infty$ .

In the current paper we seek to identify the uncertain parameter in the plant by minimizing  $\mu_\theta(t)$  over  $\theta \in \Theta$ . To this effect, a KF is designed based on a model of plant assuming  $\theta = \theta_0$ . The residuals of the KF are used to compute  $\mu_\theta(t)|_{\theta=\theta_0}$ . Then, the derivative of  $\mu_\theta(t)$  with respect to  $\theta$  is computed (for  $\theta = \theta_0$ ) and a new estimate of  $\hat{\theta}$  (denoted by  $\theta_1$ ) is computed as

$$\theta_n = \theta_{n-1} - \gamma \nabla \mu_\theta(t)|_{\theta=\theta_{n-1}}, \quad (n = 1, 2, \dots) \quad (19)$$

where  $\gamma$  is the minimization step size and  $\nabla \mu_\theta(t)|_{\theta=\theta_{n-1}}$  is the gradient of  $\mu_\theta$  with respect to  $\theta$ , evaluated at  $\theta = \theta_{n-1}$ . Then, a new KF is designed based on a model of plant assuming  $\theta = \theta_n$ . We should highlight that (19) is updated with a slower rate than the sampling time of the system. The update rate in (19) depends on the effective convergence time of the dynamic Riccati equation (given in 16) and the dynamics of the system. In the next section we consider the problem of computing  $\nabla \mu_\theta(t)$ .

#### IV. GRADIENT EVALUATION

Defining  $g(\theta, \tau) = \frac{1}{2} [\tilde{y}_\theta^T(\tau) S_\theta^{-1}(\tau) \tilde{y}_\theta(\tau) + \log |S_\theta(\tau)|]$ , (18) is given by

$$\mu_\theta(t) = \sum_{\tau=1}^{\tau=t} g(\theta, \tau). \quad (20)$$

In order to evaluate  $\nabla \mu_\theta(t)$ , we first study  $\nabla g(\theta, t)$  (the gradient of  $g(\theta, t)$  with respect to  $\theta$ ). is straightforward to show that

$$\frac{\partial g(\theta, t)}{\partial \theta_i} = \frac{1}{2} \frac{\partial [\tilde{y}_\theta^T(t) S_\theta^{-1}(t) \tilde{y}_\theta(t)]}{\partial \theta_i} + \frac{1}{2} \frac{\partial \log |S_\theta(t)|}{\partial \theta_i}, \quad (21)$$

where  $\theta_i$  is the  $i$ th component of  $\theta$ . The first term in the right hand side of (21) yields

$$\begin{aligned} \frac{1}{2} \frac{\partial [\tilde{y}_\theta^T(t) S_\theta^{-1}(t) \tilde{y}_\theta(t)]}{\partial \theta_i} &= \tilde{y}_\theta^T(t) S_\theta^{-1}(t) \frac{\partial \tilde{y}_\theta(t)}{\partial \theta_i} \\ &\quad - \frac{1}{2} \tilde{y}_\theta^T(t) S_\theta^{-1}(t) \frac{\partial S_\theta(t)}{\partial \theta_i} S_\theta^{-1}(t) \tilde{y}_\theta(t). \end{aligned} \quad (22)$$

The second term in the right hand side of (21) can be written as

$$\frac{1}{2} \frac{\partial \log |S_\theta(t)|}{\partial \theta_i} = \frac{1}{2} \text{trace}[S_\theta^{-1}(t) \frac{\partial S_\theta(t)}{\partial \theta_i}]. \quad (23)$$

We now need to compute  $\frac{\partial \tilde{y}_\theta(t)}{\partial \theta_i}$  and  $\frac{\partial S_\theta(t)}{\partial \theta_i}$  in order to evaluate  $\nabla \mu_\theta(t)$ . Using (16) it follows that

$$\begin{aligned} \frac{\partial \tilde{y}_\theta(t)}{\partial \theta_i} &= \frac{\partial}{\partial \theta_i} [y(t) - C_\theta \hat{x}_\theta(t|t-1)] \\ &= -\frac{\partial C_\theta}{\partial \theta_i} \hat{x}_\theta(t|t-1) - C_\theta \frac{\partial \hat{x}_\theta(t|t-1)}{\partial \theta_i}. \end{aligned} \quad (24)$$

The term  $\frac{\partial \hat{x}_\theta(t|t-1)}{\partial \theta_i}$  is called the Kalman filter sensitivity equation [14], [18]. Using (16a), it can be shown that

$$\frac{\partial \hat{x}_\theta(t+1|t)}{\partial \theta_i} = A_\theta^{cl}(t) \frac{\partial \hat{x}_\theta(t|t-1)}{\partial \theta_i} + \varpi_\theta^i(t), \quad (25)$$

where  $A_\theta^{cl}(t) = A_\theta - A_\theta H_\theta(t) C_\theta$  and

$$\varpi_\theta^i(t) = \frac{\partial A_\theta^{cl}(t)}{\partial \theta_i} \hat{x}_\theta(t|t-1) + \frac{\partial [A_\theta H_\theta(t)]}{\partial \theta_i} y(t). \quad (26)$$

All terms in equation (26) are computed and available to propagate the Kalman filter sensitivity equation, given by (25), except the term  $\frac{\partial H_\theta(t)}{\partial \theta_i}$ . Computing the derivatives of both sides of (16b) with respect to  $\theta_i$  we obtain

$$\begin{aligned} \frac{\partial H_\theta(t)}{\partial \theta_i} &= \frac{\partial \Sigma_\theta(t|t-1)}{\partial \theta_i} C_\theta^T S_\theta^{-1}(t) + \Sigma_\theta(t|t-1) \frac{\partial C_\theta^T}{\partial \theta_i} S_\theta^{-1}(t) \\ &\quad - \Sigma_\theta(t|t-1) C_\theta^T S_\theta^{-1}(t) \frac{\partial S_\theta(t)}{\partial \theta_i} S_\theta^{-1}(t). \end{aligned} \quad (27)$$

Similarly, differentiating both sides of (16c) with respect to  $\theta_i$  yields

$$\begin{aligned} \frac{\partial S_\theta(t)}{\partial \theta_i} &= C_\theta \frac{\partial \Sigma_\theta(t|t-1)}{\partial \theta_i} C_\theta^T \\ &\quad + \frac{\partial C_\theta}{\partial \theta_i} \Sigma_\theta(t|t-1) C_\theta^T + C_\theta \Sigma_\theta(t|t-1) \frac{\partial C_\theta^T}{\partial \theta_i} \end{aligned} \quad (28)$$

At this stage, only the term  $\frac{\partial \Sigma_\theta(t|t-1)}{\partial \theta_i}$  remains to be computed in order to complete this section. Using (16d) it follows that

$$\begin{aligned} \frac{\partial \Sigma_\theta(t+1|t)}{\partial \theta_i} &= \frac{\partial A_\theta}{\partial \theta_i} \Sigma_\theta(t|t-1) A_\theta^T + A_\theta \Sigma_\theta(t|t-1) \frac{\partial A_\theta^T}{\partial \theta_i} \\ &\quad + A_\theta \frac{\partial \Sigma_\theta(t|t-1)}{\partial \theta_i} A_\theta^T - \frac{\partial A_\theta}{\partial \theta_i} H_\theta(t) S_\theta(t) H_\theta^T(t) A_\theta^T \\ &\quad + \frac{\partial G_\theta Q G_\theta^T}{\partial \theta_i} - A_\theta H_\theta(t) S_\theta(t) H_\theta^T(t) \frac{\partial A_\theta^T}{\partial \theta_i} \\ &\quad - A_\theta H_\theta(t) \frac{\partial S_\theta(t)}{\partial \theta_i} H_\theta^T(t) A_\theta^T \\ &\quad - A_\theta \frac{\partial H_\theta(t)}{\partial \theta_i} S_\theta(t) H_\theta^T(t) A_\theta^T \\ &\quad - A_\theta H_\theta(t) S_\theta(t) \frac{\partial H_\theta^T(t)}{\partial \theta_i} A_\theta^T, \end{aligned} \quad (29)$$

Recalling from (16b) that  $H_\theta(t) S_\theta(t) = \Sigma_\theta(t|t-1) C_\theta^T$  and  $S_\theta(t) H_\theta^T(t) = C_\theta \Sigma_\theta(t|t-1)$ , and using (27) for  $\frac{\partial H_\theta(t)}{\partial \theta_i}$  we obtain

$$\begin{aligned} \frac{\partial \Sigma_\theta(t+1|t)}{\partial \theta_i} &= \frac{\partial A_\theta}{\partial \theta_i} \Sigma_\theta(t|t-1) A_\theta^T + A_\theta \Sigma_\theta(t|t-1) \frac{\partial A_\theta^T}{\partial \theta_i} \\ &\quad + A_\theta \frac{\partial \Sigma_\theta(t|t-1)}{\partial \theta_i} A_\theta^T - \frac{\partial A_\theta}{\partial \theta_i} \Sigma_\theta(t|t-1) C_\theta^T H_\theta^T(t) A_\theta^T \\ &\quad + \frac{\partial G_\theta Q G_\theta^T}{\partial \theta_i} - A_\theta H_\theta(t) C_\theta \Sigma_\theta(t|t-1) \frac{\partial A_\theta^T}{\partial \theta_i} \\ &\quad - A_\theta H_\theta(t) \frac{\partial S_\theta(t)}{\partial \theta_i} H_\theta^T(t) A_\theta^T \\ &\quad - A_\theta \frac{\partial \Sigma_\theta(t|t-1)}{\partial \theta_i} C_\theta^T H_\theta^T(t) A_\theta^T \\ &\quad - A_\theta \Sigma_\theta(t|t-1) \frac{\partial C_\theta^T}{\partial \theta_i} H_\theta^T(t) A_\theta^T \\ &\quad + A_\theta \Sigma_\theta(t|t-1) C_\theta^T S_\theta^{-1}(t) \frac{\partial S_\theta(t)}{\partial \theta_i} H_\theta^T(t) A_\theta^T \\ &\quad - A_\theta H_\theta(t) C_\theta \frac{\partial \Sigma_\theta(t|t-1)}{\partial \theta_i} A_\theta^T, \\ &\quad - A_\theta H_\theta(t) \frac{\partial C_\theta}{\partial \theta_i} \Sigma_\theta(t|t-1) A_\theta^T, \\ &\quad + A_\theta H_\theta(t) \frac{\partial S_\theta(t)}{\partial \theta_i} S_\theta^{-1}(t) C_\theta \Sigma_\theta(t|t-1) A_\theta^T. \end{aligned} \quad (30)$$

Substituting for  $\frac{\partial S_\theta(t)}{\partial \theta_i}$  from (28) and reordering the terms, we obtain the dynamic Riccati sensitivity equations [18], [19] as

$$\frac{\partial \Sigma_\theta(t+1|t)}{\partial \theta_i} = A_\theta^{cl}(t) \frac{\partial \Sigma_\theta(t|t-1)}{\partial \theta_i} A_\theta^{clT}(t) + \varphi_\theta^i(t) + \varphi_\theta^{iT}(t), \quad (31)$$

where

$$\begin{aligned} \varphi_\theta^i(t) &= \frac{\partial A_\theta}{\partial \theta_i} \Sigma_\theta(t|t-1) A_\theta^{clT}(t) + \frac{\partial G_\theta}{\partial \theta_i} Q G_\theta^T \\ &\quad - A_\theta H_\theta(t) \frac{\partial C_\theta}{\partial \theta_i} \Sigma_\theta(t|t-1) A_\theta^{clT}(t). \end{aligned} \quad (32)$$

To summarize this section we provide, in the following, a procedure by which  $\nabla \mu_\theta(t)$  is computed. At each sampling time the following algorithm enables us to compute  $\nabla g(\theta, t)$ .

Then, by using (20) we can evaluate  $\nabla\mu_\theta(t)$ .

**Algorithm**

**Input Data:**  $A_\theta, G_\theta, C_\theta, H_\theta(t), S_\theta(t), \Sigma_\theta(t|t-1), Q, y(t)$ , and  $\hat{x}_\theta(t|t-1)$ .

**Output Data:**  $\nabla g(\theta, t)$ .

**Process:**

For each component of  $\theta$ ,

- 1) Compute  $\varphi_\theta^i(t)$  in (32) and propagate (31).
- 2) Compute  $\frac{\partial S_\theta(t)}{\partial \theta_i}$  using (28).
- 3) Compute  $\frac{\partial H_\theta(t)}{\partial \theta_i}$  using (27).
- 4) Compute  $\varpi_\theta^i(t)$  in (26) and propagate (25).
- 5) Compute  $\frac{\partial \hat{y}_\theta(t)}{\partial \theta_i}$  using (24).
- 6) Compute  $\frac{\partial g(\theta, t)}{\partial \theta_i}$  using (21), (22), and (23).

## V. EXPERIMENTAL RESULTS

The proposed adaptive wave filter was tested using the model vessel Cybership III, at the Marine Cybernetic Laboratory (MCLab) of the Department of Marine Technology at the Norwegian University of Science and Technology (NTNU). The performance of the parameter identification methodology was evaluated under different sea conditions produced by a hydraulic wave maker. The DWF was identified using the proposed methodology and the wave filtering was performed using the Kalman wave filter tuned according to the identified DWF.

### A. Overview of the Cybership III

CyberShip III is a 1:30 scaled model of an offshore vessel operating in the North Sea. Fig. 1 shows the vessel at the basin in the MCLab and table II presents the main parameters of the model and full scale vessel.

TABLE II  
MODEL MAIN PARAMETERS

|  | Model    | Full Scale |
|--|----------|------------|
| Overall Length                                   | 2.275 m  | 68.28 m    |
| Length between perpendiculars                    | 1.971 m  | 59.13 m    |
| Breadth  | 0.437 m  | 13.11 m    |
| Breadth at water line                            | 0.437 m  | 13.11 m    |
| Draught  | 0.153 m  | 4.59 m     |
| Draught front perpendicular                      | 0.153 m  | 4.59 m     |
| Draught aft. perpendicular                       | 0.153 m  | 4.59 m     |
| Depth to main deck                               | 0.203 m  | 6.10 m     |
| Weight (hull)                                    | 17.5 kg  | Unknown    |
| Weight (normal load)                             | 74.2 kg  | 22.62 tons |
| Longitudal center of gravity                     | 100 cm   | 30 m       |
| Vertical center of gravity                       | 19.56 cm | 5.87 m     |
| Propulsion motors max shaft power (6% gear loss) | 81 W     | 3200 HP    |
| Tunnel thruster max shaft power (6% gear loss)   | 27 W     | 550 HP     |
| Maximum Speed                                    | Unknown  | 11 knots   |

Cybership III is equipped with two pods located at the aft. A tunnel thruster and an azimuth thruster are installed in the bow.<sup>3</sup> It has a mass of  $m = 75$  (kg), length of

<sup>3</sup>For technical reasons, in this experiment the tunnel thruster was deactivated.



Fig. 1. Cybership III.

$L = 2.27$  (m) and breadth of  $B = 0.4$  (m). The main parameters of the model are presented in Table II. The internal hardware architecture is controlled by an onboard computer which can communicate with onshore PC through a WLAN. The PC onboard the ship uses the QNX real-time operating system (target PC). The parameter identification, adaptive wave filter, and control systems described before were developed on a PC in the control room (host PC) under Simulink/Opal and downloaded to the target PC using automatic C-code generation and wireless Ethernet. The motion capture unit (MCU), installed in the MCLab, provides Earth-fixed position and heading of the vessel. The MCU consists of onshore 3-cameras mounted on the towing carriage and a marker mounted on the vessel. The cameras emit infrared light and receive the light reflected from a marker on the vessel. To simulate the different sea conditions, a hydraulic wave maker system was used. It consists of a single flap covering the whole breadth of the basin, and a computer controlled motor, moving a flap. The device can produce regular and irregular waves with different spectra. We have used the JONSWAP spectrum to simulate the different sea conditions for our experiment.

Due to limited computation power of the PC onboard the ship we implemented the proposed methodology using a steady state KF. In this case,  $H_\theta$  and  $S_\theta$  are independent of time and the equations above simplify notably and can be implemented easier on computers with limited computation power. Using a steady state KF, the recursive Riccati sensitivity equations in (31) simplify to a discrete Lyapunov equation given by

$$\frac{\partial \Sigma_\theta}{\partial \theta_i} = A_\theta^{cl} \frac{\partial \Sigma_\theta}{\partial \theta_i} A_\theta^{clT} + \varphi_\theta^i + \varphi_\theta^{iT}. \quad (33)$$

Moreover, we assumed that the DWF in surge, sway, and heading are equal, i.e.  $\omega_{01} = \omega_{02} = \omega_{03} = \omega$ . During the numerical simulations we found that the proposed parameter identification technique is sensitive to initial value of the uncertain parameter. To alleviate this problem, we used four KFs designed based on four different representative values of the uncertain parameter (uniformly distributed in the uncertain parameter space,  $\{0.672, 0.954, 1.236, 1.518\}$ ) and the performance index of each KF (given by (18)) was evaluated. The representative value of the KF with minimum performance index was selected as the initial value for the parameter identification algorithm.

Fig. 2 shows the results of an experiment where the wave maker system simulates a moderate sea state with  $\omega = 0.8$

(rad/sec). In this experiment we updated the DWF estimation every 25 seconds. During the first 25 seconds, four KFs ran in parallel and at time  $t = 25$  (sec) the KF tuned for  $\omega = 0.9540$  (rad/sec) had the minimum performance index value; therefore,  $\omega = 0.954$  (rad/sec) was selected as the initial value for parameter identification. Throughout the experiment a multivariable PID controller was used for station keeping. The first (upper) sub-figure in Fig. 2 shows the wave elevation profile recorded by a probe installed five meters away from the wave maker. The second, third and fourth sub-figures in Fig. 2 show the time evolution of the positions and heading of the vessel. The last sub-figure in Fig. 2 shows the estimated DWF. The final estimate of the DWF take its value around  $\omega = 0.86$  (rad/sec) which is different from the set value of the wave maker. Later, when we estimated the power spectral density of time series of wave elevation, we found that a more accurate DWF value was  $\omega = 0.90$  (rad/sec). We suspect that the small bias in the estimation is due to a) the simplified model of plant used for identification, b) the assumption of equal DWFs in surge, sway, and heading, and c) tuning of disturbance covariances in the KFs.<sup>4</sup>

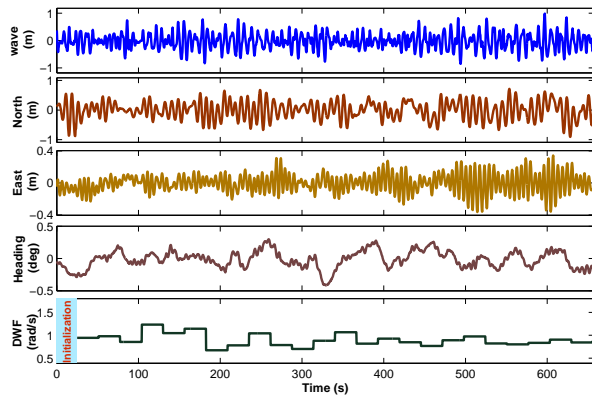


Fig. 2. Experimental results: evolution of the wave profile, the position and heading of the vessel, and the DWF estimation in moderate sea state.

## VI. CONCLUSIONS AND FUTURE RESEARCH

This paper proposed a new technique for adaptive wave filtering, with applications to DP. Its key contribution was the use of a new parameter identification technique (for estimating the sea state) in adaptive wave filtering. A numerical optimization methodology was proposed to estimate the dominant wave frequency. The estimated dominant wave frequency was used to design an adaptive Kalman filter for marine vessel adaptive wave filtering. The results were experimentally verified by model testing a DP operated ship, the Cybership III, under simulated sea condition in a towing tank. The experimental data confirms that the method developed holds promise for practical applications. Future work will include the application of the method developed to time-varying operational conditions, from calm to extreme seas.

<sup>4</sup>We should stress that we have tuned the algorithm during a few tests and Fig. 2 shows the final tuned system.

## ACKNOWLEDGMENT

We thank our colleagues A. Pedro Aguiar, J. Hespanha and Michael Athans for many discussions on adaptive estimation and control. We would also like to thank T. Wahl, Øyvind Smogeli, M. Etemaddar, E. Peymani, M. Shapouri, and B. Ommani for their generous assistance during the model tests.

## REFERENCES

- [1] J. Balchen, N. Jenssen, and S. Sælid, "Dynamic positioning using Kalman filtering and optimal control theory," in the *IFAC/IFIP Symposium On Automation in Offshore Oil Field Operation*, Bergen, Norway, 1976, pp. 183–186.
- [2] M. J. Grimble, R. J. Patton, and D. A. Wise, "The design of dynamic ship positioning control systems using stochastic optimal control theory," *Optimal Control Applications and Methods*, vol. 1, pp. 167–202, 1980.
- [3] S. Sælid, N. A. Jenssen, and J. Balchen, "Design and analysis of a dynamic positioning system based on Kalman filtering and optimal control," *IEEE Transactions on Automatic Control*, vol. 28, no. 3, pp. 331–339, 1983.
- [4] A. J. Sørensen, S. I. Sagatun, and T. I. Fossen, "Design of a dynamic positioning system using model-based control," *Journal of Control Engineering Practice*, vol. 4, no. 3, pp. 359–368, 1996.
- [5] G. Torsetnes, J. Jouffroy, and T. I. Fossen, "Nonlinear dynamic positioning of ships with gain-scheduled wave filtering," in *Proc. IEEE Conference on Decision and Control (CDC'04)*, Paradise Iceland, Bahamas, 2004.
- [6] T. D. Nguyen, A. J. Sørensen, and S. T. Quek, "Design of hybrid controller for dynamic positioning from calm to extreme sea conditions," *Automatica*, vol. 43, no. 5, pp. 768–785, 2007.
- [7] V. Hassani, A. J. Sørensen, A. M. Pascoal, and A. P. Aguiar, "Multiple model adaptive wave filtering for dynamic positioning of marine vessels," in *Proc. ACC'12 - American Control Conference*, Montreal, Canada, 2012.
- [8] V. Hassani, A. J. Sørensen, and A. M. Pascoal, "Robust dynamic positioning of offshore vessels using mixed- $\mu$  synthesis, part I: Designing process; part II: Simulation and experimental results," in *Proc. ACOOG 2012 - IFAC Workshop on Automatic Control in Offshore Oil and Gas Production*, Trondheim, Norway, 2012.
- [9] —, "A novel methodology for robust dynamic positioning of marine vessels: Theory and experiments," in *Proc. ACC'13 - American Control Conference*, Washington, DC, USA, 2013.
- [10] A. J. Sørensen, "A survey of dynamic positioning control systems," *Annual Reviews in Control*, vol. 35, pp. 123–136, 2011.
- [11] T. I. Fossen, *Handbook of Marine Craft Hydrodynamics and Motion Control*. Chichester, UK: John Wiley & Sons, Ltd, 2011.
- [12] T. I. Fossen and J. P. Strand, "Passive nonlinear observer design for ships using lyapunov methods: Full-scale experiments with a supply vessel," *Automatica*, vol. 35, pp. 3–16, 1999.
- [13] W. G. Price and R. E. D. Bishop, *Probabilistic Theory of Ship Dynamics*. London, UK: Chapman and Hall, 1974.
- [14] B. D. O. Anderson and J. B. Moore, *Optimal Filtering*. New Jersey, USA: Prentice-Hall, 1979.
- [15] V. Hassani, A. P. Aguiar, A. M. Pascoal, and M. Athans, "A performance based model-set design strategy for multiple model adaptive estimation," in *ECC'09 - European Control Conference*, Budapest, Hungary, 2009.
- [16] Y. Baram and N. Sandell, "An information theoretic approach to dynamical systems modeling and identification," *IEEE Trans. on Automat. Contr.*, vol. 23, pp. 61–66, 1978.
- [17] V. Hassani, J. Hespanha, M. Athans, and A. M. Pascoal, "Stability analysis of robust multiple model adaptive control," in *Proc. of The 18th IFAC World Congress*, Milan, Italy, 2011.
- [18] N. R. Sandell and K. I. Yared, "Maximum likelihood identification of state space models for linear dynamic systems," Electronic Systems Laboratory, Dept. of Electrical Engineering and Computer Science, Massachusetts Institute of Technology, Tech. Rep. Report ESL-R-814, 1978.
- [19] N. K. G. R. K. Mehra, "Computational aspects of maximum likelihood estimation and reduction in sensitivity function calculations," *IEEE Trans. on Automat. Contr.*, vol. 19, no. 6, pp. 774–783, 1974.